Permissive expansion and homing of adoptively transferred T cells in tumor-bearing hosts.

Perez, C., Jukica, A., Listopad, J.J., Anders, K., Kuehl, A.A., Loddenkemper, C., Blankenstein, T., Charo, J.

International Journal of Cancer
2015 MMM ; 137(2): 359-371
doi: http://dx.doi.org/10.1002/ijc.29401
Publisher: Wiley-Blackwell

Permissive expansion and homing of adoptively transferred T cells in tumor-bearing hosts

C. Perez[1,5], A. Jukica[1,†], J. J. Listopad[1,†], Kathleen Anders[1], A. A. Kühl[2], C. Loddenkemper[3,6], T. Blankenstein[1,4] and J. Charo[1,7]

[1] Max-Delbrück-Center for Molecular Medicine, Robert-Rössle Str. 10, 13125 Berlin, Germany

[2] Department of Medicine I for Gastroenterology, Infectious Disease and Rheumatology, and

[3]Institute of Pathology, Charité Campus Benjamin Franklin, Hindenburgdamm 30, 12200 Berlin, Germany

[4] Institute of Immunology, Charité Campus Buch, Lindenberger Weg 80, 13125 Berlin, Germany

[5] Present address: Oncology Institute of the Cardinal Bernardin Cancer Center, Loyola University Chicago, 216 S. First Avenue, Maywood, IL 60153, USA

[6] Present address: Gemeinschaftspraxis fuer Pathologie PathoTres, Teltowkanalstr. 2, 12247 Berlin, Germany

[7] Present address: Roche Pharma Research and Early Development, Roche Innovation Center Basel, F. Hoffmann-La Roche Ltd., Grenzacherstrasse 124, 4070 Basel, Switzerland,

[†] A. J. and J. L. contributed equally to this work

Short title: Expansion and homing of adoptively transferred T cells to tumors

Corresponding author: Jehad Charo, DTA Oncology, Roche Pharma Research and Early Development, Roche Innovation Center Basel, F. Hoffmann-La Roche Ltd., Grenzacherstrasse 124, 4070 Basel, Switzerland, Phone: +41 61 687 00 47, Fax: +41 61 688 03 55, e-mail: jehad.charo@roche.com

Key words: Cancer, adoptive therapy, bioluminescence imaging, CD8 T cells

Abbreviations: Alb (Albumin), BLI (Bioluminescence imaging), FLuc (Firefly luciferase), LTL (LoxTagLuc), Luc (luciferase), Ova (ovalbumin), RLuc (Renilla luciferase), R-OT (RLuc-OT I), R-TCRI (RLuc-TCRI), RT-Rack (RLuc T cell tracking), Tag (SV40 Large T antigen), TagLuc (fusion of Tag and Luc)

Article category: Tumor immunology

Novelty and impact

The ability of adoptively transferred T cells to expand, and home to tumors are essential steps for successful therapy. Using mouse models that differed in tumor burden, nature of targeted antigen and tumor location, we found that neither ignorance nor immunological exclusion prevented the *in vivo* response of transferred T cells. In contrast, functionally active T cells with low expression of the inhibitory receptor PD1 were mainly observed in the immunodeficient and target-antigen-negative tumor-bearing hosts.

Abstract

Activated T cells expressing endogenous or transduced TCRs are two cell types currently used in clinical adoptive T-cell therapy. The ability of these cells to recognize their antigen, expand, and traffic to the tumor site are the initial steps necessary for successful therapy. In this study, we used *in vivo* bioluminescent imaging (BLI) of Renilla luciferase (RLuc) expressing T cells to evaluate the ability of adoptively transferred T cells to survive, expand and home to tumor site *in vivo*. Using this method, termed RT-Rack (Rluc T cell tracking), we followed T-cell response against tumors *in vivo*. Expansion and homing of adoptively transferred T cells were antigen dependent, but independent of the host immune status. Moreover, we successfully detected T-cell response to small and large tumors, including autochthonous liver tumors. The adoptively transferred T cells were not ignorant or excluded in a partially tolerant host, which expressed low level of the target in the periphery. Using T cell receptor-engineered T cells, we showed the ability of these cells to respond in tumor-bearing hosts by expanding and homing to the tumor site. In all these models, the host immune status, the nature of the tumor or of the antigen, the tumor size, and the presence of the targeted antigen in the periphery did not prevent the adoptively transferred T cells from responding by expanding and homing to the tumor. However, T cells had higher expression of the inhibitory receptor PD1 and reduced functional activity when a self-antigen was targeted.

Introduction

Adoptive T-cell therapy is currently used in the clinic to treat malignancies [1-7]. However, limited expansion, poor trafficking, and little accumulation of adoptively transferred T cells at the tumor site were suggested to constrain successful therapy. Using murine xenograft models, it has been demonstrated that enhanced trafficking of transferred T cells to the tumors can be obtained if appropriate chemokine's receptors were introduced to these T cells [8-10]. However, whether syngeneic tumors, including autochthonous tumors, are ignored or can be sufficiently detected *in vivo* using adoptively transferred T cells need to be evaluated.

Different imaging techniques are available to detect cells in live mice with variable sensitivities and resolutions [11]. BLI measures the emitted photons resulting from the enzymatic activity of a luciferase upon injection of its substrate. BLI is safer and more suitable than other small animal imaging techniques when mice are to be imaged repeatedly [11-13]. BLI is sensitive and basically background free because mouse tissues do not produce detectable light [13, 14]. Different cell populations expressing different luciferases can be imaged simultaneously and discriminated based on their substrate utilization and the wavelength of the emitted light [15]. Furthermore, the acquisition time for BLI is short and up to 5 mice can be imaged in parallel, thus making BLI a high throughput *in vivo* imaging technique.

In the field of cancer immunology, BLI is used to monitor tumor growth following ectopic luciferase expression in tumor cell lines. This technique is highly sensitive, enabling the detection of as few as 1000 tumor cells expressing FLuc [16] and 1000 T cells expressing RLuc [17]. Interestingly, a clear linear correlation exists between the cell number and the imaged signal of T cells obtained from the RLuc mice [17]. Recently, transgenic mouse models were established in which expression of a luciferase is linked to the oncogene indirectly by controlled co-expression or directly as a fusion protein [18-22].

T cells are among the most sensitive cells of the immune system with their ability to detect trace amount of antigen [23]. Others and we showed that adoptively transferred antigen-specific T cells can be detected in the transplanted tumor [17, 24-28]. After injecting T cells expressing RLuc (RLuc-T), a strong T cell signal can be measured specifically from the target tumor site. Recently, more sophisticated and physiologically relevant mouse models were developed which include genetically induced or sporadic tumor mouse models. In these models, the oncogene is a self-antigen expressed at low level on healthy tissues, rendering these mice fully or partially tolerant toward the oncogene [18-22, 29-35]. Adoptively transferred T cells failed to control tumor growth in these autochthonous, self-antigen induced tumor models [19]. To evaluate whether immune exclusion mechanisms in these mice prevented the T cell response [36], we established an approach that we termed RT-Rack, for *in vivo* RLuc T cell tracking, combining the high sensitivity of T cells for their target antigen with the high sensitivity of BLI. We applied RT-Rack in various tumor-bearing mouse models, including mice with autochthonous tumors overexpressing a model self-antigen, to evaluate the capacity of adoptively transferred T cells to survive, recognize syngeneic tumor-derived antigens, expand, and traffic to tumor site *in vivo*.

Materials and Methods

Cells

EG.7F, EL-4F, 16.113F, MCA205-TagLuc and MCA205-MigFLuc were earlier described [17, 37]. 9.27P was established from 9.27 [31] from long-term *in vitro* culture followed by *in vivo* passaging in C57BL/6 mice.

Mice and tumor models

C57BL/6 albino (B6/Albino) mice (C57Bl/6-Tyr$^{c\text{-}Brd}$) were injected subcutaneously (s.c.) either with 2x10^6 EG.7F or with 3-10x10^6 9.27P cells. In the spectral unmixing experiments, B6/Albino mice were injected with 2x10^6 EG.7F in the right side of the mouse and with 2x10^6 EL-4F in the left side of the mice. Rag$^{-/-}$ albino mice (including Rag1$^{-/-}$ or Rag2$^{-/-}$ mice [17]) were injected s.c. with either 3-10x10^6 9.27P, or with 10x10^6 16.113F cells. For the experimental metastasis model, Rag$^{-/-}$ mice were injected intravenously (i.v.) with 2x10^5 MCA205-TagLuc or MCA205-MigFLuc cells [38]. LTL mice were challenged s.c. with 3-10x^6 9.27P cells. LTL x Alb-Cre mice developing autochthonous HCC were described earlier [19, 31]. Tumor mean diameter was measured along three orthogonal axes (a, b and c) by a digital caliper and calculated as earlier described [39]. To be able to measure the smallest tumors in our study, tumor-injection-site was sprayed with 70% ethanol to enable the visualization of small palpable tumor nodules, which were then measured by electronic caliper. When no palpable tumor nodule was detected, similar procedures were followed using 70% ethanol spray to confirm the absence of a visible tumor nodule. Immunodeficient or immunosupressed mice (Rag$^{-/-}$ mice or mice with a large tumor burden) received antibiotic treatment. All mouse studies were carried out in accordance with institutional, state, and federal (Landesamt für Arbeitsschutz, Gesundheitsschutz und technische Sicherheit, Berlin) guidelines.

In vivo bioluminescence

Renilla luciferase (RLuc) activity was detected by retro-orbital (ro.) injection of 100 µl of coelenterazine at 1 mg/ml (Biosynth), dissolved in 30% DMSO (Sigma-Aldrich,), 70% PBS ($MgCl_2$ and $CaCl_2$ free (Invitrogen)), followed by direct measurement with the IVIS® 200 Imaging System for 1 minute, using small binning. Firefly luciferase (FLuc) activity was detected by injecting intravenously 100 µl of D-luciferin at 30 mg/ml (Biosynth), dissolved in PBS. Measurement was taken for 1 to 60 seconds using small or medium bining. Data analysis was performed using Living Image 2.6 and Living Image 4.0 software. The signal strength is depicted by a pseudocolor scale given in photon/second/cm^2/steradian (p/s/cm^2/sr).

Simultaneous dual imaging

EG.7F and EL.4F bearing B6/Albino mice were injected ro. with 100 µl of D-luciferin and, 7 minutes later, with 100 µl of coelenterazine. Successive filtered images were taken at 480, 500, 520, 540, 580, 600, 620 and 640 nm using small binning. Images taken from 480 nm to 540 nm were acquired with an exposure time of one minute while the images taken from 560 to 640 were acquired with an exposure time of 10 seconds. Alb-Cre x LTL mice were injected intravenously with 100 µl of substrate mixture containing 100 µg coelenterazine and 300 µg luciferine and imaged using similar setting as for EG.7F and EL.4F bearing B6/Albino mice, except that images taken from 560 to 640 nm were acquired with an exposure time of 1 second. RLuc and FLuc light spectra were unmixed and analyzed using Living Image 4.0 software. RLuc, FLuc and overlay signals are represented in red, green and orange respectively.

RLuc-OT-I T cell activation and treatment

Splenocytes from R-OT [17] transgenic mice were cultured in a 24-well plate at a concentration of $2x10^6$ cells/ml in presence of 1 µg/ml anti-CD3 antibody (BD Biosciences), 0.1 µg/ml anit-CD28 antibody (BD Biosciences) and 1 µg/ml SIINFEKL peptide (Biosyntan) for 24 hours in complete RPMI medium (*i.e.* RPMI-1640 Glutamax-I supplemented with 50 µM β-

mercaptoethanol, 0.1 μg/ml gentamicin (all from Invitrogen) and 10% FCS (Pan-Biotech)). 24 hours later, the medium was replaced with fresh medium containing 10 IU/ml IL-2 (interleukin-2 (Novartis)) for 3 days. $10x10^6$ cells were then injected ro. (in 100 μl PBS) into EG.7F or EG.7F and EL-4F tumor-bearing B6/Albino mice.

ChRLuc-TCRI T cell activation and treatment

ChRLuc-TCRI [17] mice were immunized by intraperitoneal injection of $1x10^7$ 16.113 cells. The spleens of these mice were harvested one week later and $CD8^+$ T cells were purified by MACS using the CD8 negative isolation kit (Miltenyi). The purity was checked by FACS after staining for CD8 and Vβ7 (Biolegend) and was about 93±4%. $1x10^6$ cells were then injected ro. (in 100 μl PBS) into 9.27P tumor bearing mice, MCA205-TagLuc bearing mice, MCA205-MigFLuc tumor bearing mice or LTL x Alb-Cre mice.

Retrovirus production

50 μl Lipofectamin™ 2000 (Invitrogen) were diluted in 1250 μl Opti-MEM (Invitrogen), incubated for 5 minutes at room temperature (RT) and mixed with 1250 μl Opti-MEM containing 7.5 μg of pCL-ECO plasmid DNA (Imgenex) mixed with 7.5 μg of MP71 plasmid DNA encoding for either TCR I (Jukica, A et al, unpublished) or with pMIG [5] as a mock control. After 20 minutes of incubation at RT, the Lipofectamin™-DNA mix was transferred onto monolayer of HEKT cells [17] (80% confluent) cultured in T75 flasks. Eight ml of complete DMEM medium (*i.e.* Dulbecco's Modified Eagle Medium supplemented with 50 μM β-mercaptoethanol, 0.1 μg/ml gentamicin (all from Invitrogen) and 10% FCS (Pan-Biotech)) were added and the cells were incubated overnight at 37°C. The medium was then replaced by fresh complete RPMI medium supplemented with 10 U/ml IL-2. Retrovirus-containing supernatants were harvested 24h and 48 hours later.

Retroviral transduction

$1x10^6$ cells/ml splenocytes from Rag-ChRLuc-OT-I mice [17] were activated *in vitro* in 24-well plates in complete RPMI medium supplemented with 1 μg/ml anti-CD3, 0.1 μg/ml anti-CD28 antibodies, 1 μg/ml SIINFEKL and 10 IU/ml IL-2. 24 hours later, the splenocytes were transduced by spinocculation. Briefly, 70% of the medium was replaced by 1 ml of retrovirus-containing supernatant supplemented with 10 μg/ml polybrene (Sigma). The plates were centrifuged at 2000 rpm for 90 minutes at 32°C. The medium was then directly exchanged with fresh complete RPMI containing 10 IU/ml IL-2 and cells were incubated at 37°C. A second transduction was done 24 hours later. One day after the last transduction, TCR I, TCR IV or GFP expression were measured by flow cytometry after co-staining with CD8 and Db/peptide I tetramers (Beckman Coulter). 16.113F-tumor bearing $Rag^{-/-}$ mice were injected with 10^5 to 10^6 T cells ro.

Immunohistology

9.27P tumors were explanted from either $Rag^{-/-}$, B6/Albino or LTL mice 2, 4 or 7 days after injection of $1x10^6$ *in vivo* activated ChRLuc-TCRI T cells. On days 4 and 7 after T-cell injection, lungs from 9.27P-bearing $Rag^{-/-}$ mice were also explanted to confirm metastasis presence. One part of each tumor and lung was fixed in formalin and embedded in paraffin, another was cryopreserved, while the third part was used to isolate Tumor-infiltrating lymphocytes (TILs) for flow cytometry analyses. Paraffin embedded sections were stained for H&E, SV40 Large T and FLuc, while CD8 staining was performed on cryosections. Staining was performed as previously described [19, 30, 31].

Isolation of tumor-infiltrating lymphocytes

9.27P tumors were cut into small fragments and digested in 2-4 ml of PBS supplemented with 78.8 μg/ml Liberase TM (Roche) and 30 U/ml DNase I (Roche) for 30 minutes at 37°C, followed by 20 minutes at room temperature. The suspension was then forced through a 40

μm cell strainer and washed twice with PBS. The TILs were then separated from the cell suspension on ficoll gradient using Ficoll-Paque™ (GE).

In vitro stimulation of TILs and splenocytes

TILs ($0.5x10^6$) were cultured with naïve C57BL/6 splenocytes ($2x10^6$) in presence of 1 μg/ml peptide I of SV40 Large T or 1 μg/ml gp33 peptides (Genquest). Splenocytes ($2x10^6$) from tumor-bearing mice were cultured in presence of 1 μg/ml peptide I of SV40 Large T or 1 μg/ml gp33 peptides. All cultures were done in 24-well plate over night at 37°C, in 1 ml complete RPMI medium, supplemented with 1 μl/ml Golgi Plug (BD).

Flow cytometry of TILs and splenocytes

TILs and splenocytes were stained *ex vivo* for cell surface expression of CD8, Vβ7, CD44, CD62L and PD-1 (Biolegend). After *in vitro* stimulation, TILs and splenocytes were stained for cell surface expression of CD8 and Vβ7, and intracellular accumulation of IFNγ and granzyme B (Biolegend). Intracellular staining of the cells was performed using the cytofix/cytoperm kit (BD Biosciences). Samples were acquired using either FACSCanto or LSR Fortesa operated by FACS Diva software (BD Biosciences). Data analysis was performed using FlowJo software (Tree Star).

Statistical analysis

Averages and standard deviations for light signals and flow cytometry values were calculated using Microsoft Excel 2007 (Microsoft Deutschland GmbH).

Results

T-cell expansion and homing are antigen dependent

We have shown earlier that T cell accumulation into large tumors is antigen specific and leads to the detection of a strong and reliable signal by BLI and confirmed the homing by flow cytometry [17]. In order to evaluate RT-Rack as a general method to measure T cell expansion and trafficking to tumor site *in vivo*, regardless of tumor burden, we first needed to visualize the co-localization of T cells and tumors by BLI. Therefore, EG.7F tumor cells expressing the model antigen ovalbumin (Ova) and its parental cell line EL-4F lacking Ova were injected on opposite flanks of C57BL/6 albino mice. Both tumor cell lines expressed FLuc, allowing us to follow their growth not only by tumor palpation but also by BLI. One week after tumor cell injection, at the day of ChRLuc-OT-I (R-OT) T cells injection, both EG.7F and EL-4F measured about 5 mm in mean diameter and had comparable FLuc signals (Fig. 1A). Within four days, EG.7F tumors were being rejected, as determined by a decrease in tumor size (data not shown). To analyze whether EG.7F and T cell signals co-localized, substrates for both FLuc and RLuc were injected simultaneously. In 4 of 7 mice, the EG.7F Fluc signal was no longer measurable at 640 nm (Fig. 1B, bottom middle panel), while the EG.7F FLuc signal could still be measured in the 3 remaining mice (Fig. 1B, bottom right panel). In the latter group, T cells and EG.7F signals co-localized, as shown by the orange color (Fig. 1C, right panel). On the opposite flank of the mice, where EL-4F tumor cells were injected, mainly the FLuc signal could be measured, as shown by a strong and predominantly green color. This confirms our earlier finding that T cell (RLuc) signal was clearly detectable from the antigen positive EG.7F tumor but not from the antigen negative EL-4F tumor (Fig. 1B). Interestingly, even in the group of mice where the EG.7F tumor signal disappeared within four days following T cell injection, a signal from the T cells was still detectable at the tumor site (Fig. 1C, middle panel).

RT-Rack detected response to large, medium, and small tumors and to unpalpable tumor cell mass

Having confirmed that RT-Rack can detect T-cell homing to antigen positive tumors, we evaluated the sensitivity of this approach by injecting RLuc-T cells into 4 groups of mice bearing decreasing EG.7F tumor burden or unpalpable EG.7F tumor cell mass.

At the day of T cell injection, tumor cells masses were either unpalpable or had a mean diameter of 1, 7 or 10 mm. This size difference correlated with the tumor specific FLuc signals (Fig. 1D). Following the injection into the tumor bearing hosts, T cells expanded, homed, and accumulated in the antigen positive tumors within 3 to 4 days and remained there for 3 more days as shown by a stable T cell signal between days 3 and 6 after T cell injection (Fig. 1E). The T cell signal then decreased, corresponding to the contraction phase of a normal immune response (Fig. 1E). Despite the difference in the sizes of targeted tumors, R-OT T cells expanded and homed to all these tumors (Fig. 1F), proving that RT-Rack is sensitive enough to detect T-cell response to small, and even unpalpable tumor cell masses *in vivo*.

9.27P tumor cells express SV40 Large T (Tag), including epitope I which is recognized by ChRLuc-TCRI (R-TCRI) T cells [31]. Groups of C57BL/6 mice were challenged s.c. with 9.27P tumor cells 14, 6 or 3 days before receiving R-TCRI T cells. Similar to the data with EG.7F tumors, RT-Rack detected T cells accumulation in these tumors efficiently despite their size differences, which was confirmed by flow cytometry (Supplementary Fig. S1, S2B, and S2D).

T cell expansion and homing was not limited by the host immune status

After evaluating RT-Rack with a model tumor antigen, we tested whether this approach could be available for detecting T cell expansion and homing toward tumors expressing other

epitopes, and whether the host immune status can influence RT-Rack's ability to detect T cell response to tumors.

LoxP-TagLuc (LTL) mice are transgenic for TagLuc, which enables the visualization of oncogene expression [19]. The expression of TagLuc in these mice is blocked by a stop cassette flanked by 2 LoxP sites, which can be deleted in the presence of Cre recombinase. Due to the leakiness of the stop cassette, LTL mice express very low level of TagLuc ubiquitously, which is detectable by BLI and are tolerant to Tag expressing tumors [19]. Immunocompetent C57BL/6, Tag-tolerant LTL or immunodeficient $Rag^{-/-}$ mice were challenged s.c. with 9.27P tumor cells. Both control and tumor-bearing mice were injected 14-18 days later with R-TCRI T cells and imaged to detect T-cell signal. The 9.27P tumors grew faster in LTL (13.1 ± 1.4 mm in mean diameter) and $Rag^{-/-}$ mice (12.3 ± 1.9 mm in mean diameter, compared to 7.9 ± 2.1 mm in mean diameter in C57BL/6 mice at day of treatment), probably due to the immune deficient or Tag tolerant environments. Therefore, these tumors were larger at these various imaging time points. R-TCRI T cells expanded and homed to the tumor sites in $Rag^{-/-}$, LTL and C57BL/6 mice (Fig. 2A-B and Supplementary Fig. S2A-C). As LTL mice have a black fur, the T cell light signal as well as the background signal are lower in these mice as compared to the albino $Rag^{-/-}$ and C57BL/6 mice [19]. Similar data were obtained by flow cytometry of TILs from tumors explanted from LTL and C57BL/6 mice and by immunohistochemistry for sections from tumors explanted from $Rag^{-/-}$ mice (Supplementary Fig. S2D-G). Moreover, the kinetics of T cell accumulation was similar in $Rag^{-/-}$ and C57BL/6 mice, starting at day 3 and peaking at day 6 (Fig. 2C). However, T cells proliferated more in $Rag^{-/-}$ mice, leading to higher signal from whole body (Fig. 2D) and secondary lymphoid organs (Fig. 2A-B) from these mice compared to C57BL/6 mice. In addition to the signals detected from the tumor and presumably secondary lymphoid organs, a specific T-cell signal was measured from the lung of the immunodeficient mice (Fig. 2B), most likely due to

T cell accumulation at the site of metastatic lesions. This was confirmed by immunohistochemistry, following staining for Tag in the lung sections from mice that received tumor challenge as compared to unchallenged mice (Fig 2E).

Interestingly, in Fig. 2B, a strong signal was imaged at the tumor rim but not from the central area. Two main reasons can explain this. The first is the necrosis in the center of the tumor, which leads to the lack of live cells expressing the targeted antigen (H2-D^b-presented Tag epitope I). The second is T-cell infiltration that is limited to the tumor edge and lack of infiltration of live tumor center. We have earlier shown that necrosis of the tumor center is induced following adoptive T cell therapy of large tumors in immunodeficient mice [37]. To better investigate this, we have analyzed sections of these tumors by immunohistochemistry. Our data confirmed that while the tumor center was composed of mainly dead cells, the T cells co-localized at the tumor edge with live tumor cells (Fig. 2F).

Adoptively transferred T cells responded to experimental metastases

Minimal residual and disseminated metastatic tumors develop at early stages of tumor development and throughout its various stages, which contribute to the high mortality rate of cancer patients [22, 40]. To evaluate whether RT-Rack can detect T-cell response to metastatic lesions, we developed an experimental bioluminescence model mimicking metastasis by injecting $Rag^{-/-}$ mice intravenously with MCA205-TagLuc, a fibrosarcoma derived from the tumor cell line MCA205 by transfection with a plasmid expressing Tag fused to FLuc (TagLuc) [37]. Experimental metastases formed within 4-7 days after tumor cell injection as detected by the FLuc activity from the lungs area (Fig. 3A-B). The presence of tumor nodules in the lungs was confirmed *ex vivo* by BLI (Fig. 3E) and by immunohistochemistry (Supplementary Fig. S3).

Five days following tumor cell injection, R-TCRI T cells were injected and mice were then imaged daily for the detection of T-cell signal. T cells expanded and accumulated in the lung area in tumor-bearing mice whereas no specific signal was detectable from tumor free control mice (Fig. 3C-F). Six days after T cell injection, mice were sacrificed and the lungs were imaged *ex vivo* to confirm the presence of T cells in the tumor-bearing lungs (Fig. 3F).

T cells, when injected i.v., reach the lungs before continuing to circulate in the blood [41]. To exclude the possibility that the T cell signal measured from the lung was due to an unspecific accumulation in this organ, $Rag^{-/-}$ mice were injected either with MCA205-TagLuc or with a control MCA205-MigFLuc tumor cells lacking the Tag protein. Upon injection of R-TCRI T cells, only mice bearing Tag-expressing tumors showed RT-Rack signal from the lung (Fig. 3G). This indicates that R-TCRI T cells expansion and accumulation at the site of metastases is antigen specific. *Ex vivo* imaging of the lungs at the peak of the signal intensity (day 6) confirmed the presence of R-TCRI T cells only when the cognate antigen was expressed by the tumor cells (Fig. 3H).

Adoptively transferred T cells responded to autochthonous hepatocellular carcinoma

We have earlier shown that crossing LTL mice with Albumin-Cre (Alb-Cre) mice leads to recombination in the liver and development of hepatocellular carcinoma (HCC) [19].

Mice transgenic for LTL and Alb-Cre as well as their control littermates (single transgenic or wild type mice) were imaged for FLuc activity to detect leakiness and HCC development. A strong signal could be measured from the liver of the LTL x Alb-Cre double transgenic mouse (Fig. 4A), indicating HCC development. The leakiness of the stop cassette, resulting in a weak expression of the transgene, could be measured only when the exposure time was increased from 1 second to 1 minute (Fig. 4A). R-TCRI T cells were injected into these mice and their survival, expansion and accumulation were followed over time by BLI. T cells

survived, expanded and preferentially accumulated at the liver site despite the weak expression of TagLuc in several normal tissues (Fig.4B, D). A weak T cell signal was nevertheless detected in these tissues in both LTL and LTL x Alb-Cre mice (Fig. 4E). Imaging FLuc and RLuc signals simultaneously confirmed the co-localization of the signals from tumor and T cells (depicted in orange in Fig. 4C). Moreover, when injected in mice bearing different tumor burden, T cell accumulation in HCC correlated with tumor burden (Fig. 4 F-H).

Adoptively transferred TCRI-engineered T cell responded to Tag expressing tumors

So far, we have evaluated the ability of T cells expressing endogenous TCR to expand and home to tumors in various mouse models. Therapeutic T cells can be produced from polyclonal T cell population by expressing a new TCR by transduction. Therefore, we evaluated whether RT-Rack can detect the response of these engineered T cells to tumors *in vivo*.

$Rag^{-/-}$ mice were injected subcutaneously with the Tag expressing tumor cell line 16.113F [17]. Mice were treated 49 days later, when the tumor measured 3 mm in mean diameter, with R-OT T cells transduced with Tag specific TCRI or with pMIG (as a mock control) retroviral vectors. On average, 25-30% of the T cells were successfully transduced as shown by flow cytometry analysis after staining with D^b/peptide I multimers specific for TCRI or by measuring GFP expression of MIG (28% and 32%, respectively) (Fig. 5A). The long waiting period before T cell injection enabled us to exclude the effects of artifactual T cell stimulation by inflammation or cross priming caused by tumor inoculum and tumor cell death [29]. These effects were reported to induce better response by the T cells [29]. T-cell expansion and accumulation were followed *in vivo* by imaging the mice for RLuc activity. TCRI transduced T cells survived, expanded and accumulated at the tumor site as shown by the strong signals

measured 7 and 9 days after T cell injection, whereas no light signal was observed at the tumor site in mice injected with mock-transduced T cells (Fig. 5B-C). Thus, RT-Rack can be combined with engineered T cells to evaluate T cell response *in vivo.*

T cells from LTL mice have reduced functional activity and increased expression of PD1

We have analyzed the profile of the T cell response in the tumor-bearing as well as tumor free $Rag^{-/-}$, C57BL/6 and LTL mice. Mice were challenged with 9.27P tumor cells and 2 weeks later received adoptive transfer of R-TCRI. One week later, splencocytes and TILs were isolated and analyzed for expression of CD44, CD62L and PD1 [42] by flow cytometry. Alternatively these T cells were stimulated over night by their cognate H2-D^b-presented epitope I peptide and stained for their ability to produce IFN-γ and granzyme B. Most TILs showed an effector memory phenotype, regardless of the immunological status or the expression of the targeted antigen (Supplementary Fig. S4). We found that T cells isolated from tumors or spleens of tumor-bearing $Rag^{-/-}$ mice have the highest effector function (IFN-γ and granzyme B production) and the lowest expression of the inhibitory receptor PD-1 (Fig. 6). In contrast, T cells isolated from tumors or spleens of tumor-bearing LTL mice showed the lowest effector function (IFN-γ and granzyme B production) and the highest expression of the inhibitory receptor PD-1 (Fig. 6).

Discussion

Antigen recognition, expansion, and homing of antigen-specific T cells to tumor sites are the initial steps necessary for the success of adoptive T cell therapy. In this study, we described an approach to detect the response of adoptively transferred T cells over time *in vivo*. We analyzed *in vivo* the impact of the antigen environment, the influence of tumor origin, and the nature of TCR expression on T-cell response by BLI. Using RLuc transgenic T cells enabled us to follow the T-cell signal repeatedly for 2-3 weeks *in vivo*. Antigen specific RLuc T cells homed to antigen positive, but not antigen negative tumors. The host environment contributes to the ability of T cells to survive and expand [43]. Nevertheless, RT-Rack detected T-cell response independently of the host immune status. At the peak of the signal, we could detect 3 to 4 fold higher signal from the tumor site in the immunodeficient as compared to the immunocompetent mice. The more prominent T cell accumulation at the tumor sites in $Rag^{-/-}$ mice might have reflected the difference in the tumor size between $Rag^{-/-}$ and C57BL/6 mice or lack of competition by the endogenous T cells. Occasional signals measured from the secondary lymphoid organs could be due to T cell accumulation in these organs or to detection of metastases. Intravenous injection of the fibrosarcoma cell line MCA205 experimentally mimicked metastases development [38]. RT-Rack detected T-cell response to these tumors only when the MCA205 expressed the target antigen Tag.

RT-Rack measured T-cell response not only to transplantable tumors and experimental metastasis, but also toward autochthonous tumors expressing the targeted Tag as a model of self-antigen. LTL x Alb-Cre mice develop HCC after a latency of 3 to 4 months [19]. HCC in these mice expressed FLuc enabling the confirmation of T-cell homing to the tumor by RT-Rack. Following injection, RT-Rack localized T-cells homing to the HCC, even as the target antigen was also expressed at low level by normal non-transformed cells [19], a characteristic common for most of the targeted cancer antigens [44]. Without pre-treatment of the host, such as

lymphodepletion, T cells successfully expanded and homed to the primary tumor. The presence of the targeted Tag at low level in the periphery did not prevent preferential T cell recognition of the tumor. This excludes the possibility that the tumor and the immunotolerant environment of the host toward Tag-specific T cells lead to T cell exclusion in this model, a mechanism proposed to explain the failure of therapeutic T cells in controlling tumor growth [36]. Notably, the intensity of the RLuc signal, representing T cell homing to the tumor, correlated with tumor burden. Interestingly, T cells were able to survive and detect an overexpressed self-antigen in this HCC mouse model, where the tumor is growing in an organ described as a graveyard for T cells [45]. In Fig 4C, the T-cell signal was detected from the whole tumor area. This signal co-localized, to a similar extent, with the tumor-cell signal in some areas (depicted by the orange color) or was stronger or weaker in other areas of the liver. This variation might reflect the density of the antigen or the cells presenting it at the imaging time. Nonetheless, the T-cell signal emanated from the whole area where the tumor signal did. T cells transduced to express the TCR specific for the peptide I of Tag successfully expanded and homed to tumors. It is therefore possible to apply the RT-Rack technique to study other tumor models, where TCR transgenic mice are not yet available, and possibly to other diseases, such as viral, bacterial, or parasitic infections [3, 6]. Moreover, the T cell engineering technology enables the possibility of the targeting of several epitopes or tumor associated antigens in parallel, for example by using TCRs recognizing two different epitopes of the same antigen. Following therapy with these T cells, it will be possible to compare *in vivo* the T cell response guided by either receptors.

The background light signal of RLuc substrate, emanating from the liver, was reported to be due to the autooxidation of the substrate [46]. Nevertheless, the signal was far weaker than the specific RT-Rack signal from the T cells accumulating in the tumor.

We evaluated the phenotypic and functional characteristic of the TILs isolated from tumor growing in immunodeficient antigen-negative $Rag^{-/-}$ mice as compared to immunocompetent mice expressing (LTL) or not (C57BL/6) the targeted tumor antigen. Our data indicated that TILs from the tumors explanted from antigen-negative and immunodeficient mice have the highest effector function and the lowest expression level of the inhibitory receptor PD1. In contrast, TILs from the tumors explanted from antigen-expressing and immunocompetent mice have the highest effector function and the lowest expression level of the inhibitory receptor PD1. We have earlier shown that Tag-expressing tumors can be rejected by adoptive T cell therapy in $Rag^{-/-}$, but not LTL mice [17, 19]. Therefore, our data show that the limiting step in this model of adoptive T cell therapy is not survival, target antigen recognition, proliferation or homing of the adoptively transferred T cells. Rather, the limiting step is the ability of these cells to differentiate into fully effector T cells that express low level of the inhibitory receptor PD1.

Acknowledgement

The authors thank Dr. G. Willimsky and B. Horrigan for the critical reading of this manuscript. We also thank M. Hensel, S. Spieckermann, M. Babka, and S. Kupsch for their excellent technical assistance and D. Tarak and R. Manteufel for their help by taking care of the mice. This work was supported by the Deutsche Forschungsgemeinschaft Transregio-Sonderforschungsbereich TR36 (J. C. and T. B.), the Deutsche Krebshilfe (J. C. and T. B.) and the European Community program FP6 “ATTACK” (T. B.).

References

1. Jensen MC, Riddell SR. Design and implementation of adoptive therapy with chimeric antigen receptor-modified T cells. *Immunol Rev* 2014;**257**: 127-44.
2. Kunert A, Straetemans T, Govers C, Lamers C, Mathijssen R, Sleijfer S, Debets R. TCR-Engineered T Cells Meet New Challenges to Treat Solid Tumors: Choice of Antigen, T Cell Fitness, and Sensitization of Tumor Milieu. *Front Immunol* 2013;**4**: 363.
3. Restifo NP, Dudley ME, Rosenberg SA. Adoptive immunotherapy for cancer: harnessing the T cell response. *Nat Rev Immunol* 2012;**12**: 269-81.
4. Rosenberg SA. Raising the bar: the curative potential of human cancer immunotherapy. *Sci Transl Med* 2012;**4**: 127ps8.
5. Charo J, Finkelstein SE, Grewal N, Restifo NP, Robbins PF, Rosenberg SA. Bcl-2 overexpression enhances tumor-specific T-cell survival. *Cancer Res* 2005;**65**: 2001-8.
6. Morgan RA, Dudley ME, Wunderlich JR, Hughes MS, Yang JC, Sherry RM, Royal RE, Topalian SL, Kammula US, Restifo NP, Zheng Z, Nahvi A, et al. Cancer regression in patients after transfer of genetically engineered lymphocytes. *Science* 2006;**314**: 126-9.
7. Blohm U, Potthoff D, van der Kogel AJ, Pircher H. Solid tumors "melt" from the inside after successful CD8 T cell attack. *Eur J Immunol* 2006;**36**: 468-77.
8. Di Stasi A, De Angelis B, Rooney CM, Zhang L, Mahendravada A, Foster AE, Heslop HE, Brenner MK, Dotti G, Savoldo B. T lymphocytes coexpressing CCR4 and a chimeric antigen receptor targeting CD30 have improved homing and antitumor activity in a Hodgkin tumor model. *Blood* 2009;**113**: 6392-402.
9. Kershaw MH, Wang G, Westwood JA, Pachynski RK, Tiffany HL, Marincola FM, Wang E, Young HA, Murphy PM, Hwu P. Redirecting migration of T cells to chemokine secreted from tumors by genetic modification with CXCR2. *Hum Gene Ther* 2002;**13**: 1971-80.
10. Craddock JA, Lu A, Bear A, Pule M, Brenner MK, Rooney CM, Foster AE. Enhanced tumor trafficking of GD2 chimeric antigen receptor T cells by expression of the chemokine receptor CCR2b. *J Immunother* 2010;**33**: 780-8.
11. Lyons SK. Advances in imaging mouse tumour models in vivo. *J Pathol* 2005;**205**: 194-205.
12. Willmann JK, van Bruggen N, Dinkelborg LM, Gambhir SS. Molecular imaging in drug development. *Nat Rev Drug Discov* 2008;**7**: 591-607.
13. O'Neill K, Lyons SK, Gallagher WM, Curran KM, Byrne AT. Bioluminescent imaging: a critical tool in pre-clinical oncology research. *J Pathol* 2010;**220**: 317-27.
14. Zhao H, Doyle TC, Coquoz O, Kalish F, Rice BW, Contag CH. Emission spectra of bioluminescent reporters and interaction with mammalian tissue determine the sensitivity of detection in vivo. *J Biomed Opt* 2005;**10**: 41210.
15. Gammon ST, Leevy WM, Gross S, Gokel GW, Piwnica-Worms D. Spectral unmixing of multicolored bioluminescence emitted from heterogeneous biological sources. *Anal Chem* 2006;**78**: 1520-7.
16. Edinger M, Cao YA, Hornig YS, Jenkins DE, Verneris MR, Bachmann MH, Negrin RS, Contag CH. Advancing animal models of neoplasia through in vivo bioluminescence imaging. *Eur J Cancer* 2002;**38**: 2128-36.
17. Charo J, Perez C, Buschow C, Jukica A, Czeh M, Blankenstein T. Visualizing the dynamic of adoptively transferred T cells during the rejection of large established tumors. *Eur J Immunol* 2011;**41**: 3187-97.
18. Vooijs M, Jonkers J, Lyons S, Berns A. Noninvasive imaging of spontaneous retinoblastoma pathway-dependent tumors in mice. *Cancer Res* 2002;**62**: 1862-7.

19. Buschow C, Charo J, Anders K, Loddenkemper C, Jukica A, Alsamah W, Perez C, Willimsky G, Blankenstein T. In vivo imaging of an inducible oncogenic tumor antigen visualizes tumor progression and predicts CTL tolerance. *J Immunol* 2010;**184**: 2930-8.
20. Liao CP, Zhong C, Saribekyan G, Bading J, Park R, Conti PS, Moats R, Berns A, Shi W, Zhou Z, Nikitin AY, Roy-Burman P. Mouse models of prostate adenocarcinoma with the capacity to monitor spontaneous carcinogenesis by bioluminescence or fluorescence. *Cancer Res* 2007;**67**: 7525-33.
21. Lyons SK, Meuwissen R, Krimpenfort P, Berns A. The generation of a conditional reporter that enables bioluminescence imaging of Cre/loxP-dependent tumorigenesis in mice. *Cancer Res* 2003;**63**: 7042-6.
22. Edinger M, Cao YA, Verneris MR, Bachmann MH, Contag CH, Negrin RS. Revealing lymphoma growth and the efficacy of immune cell therapies using in vivo bioluminescence imaging. *Blood* 2003;**101**: 640-8.
23. Davis MM, Krogsgaard M, Huse M, Huppa J, Lillemeier BF, Li QJ. T cells as a self-referential, sensory organ. *Annu Rev Immunol* 2007;**25**: 681-95.
24. Dubey P, Su H, Adonai N, Du S, Rosato A, Braun J, Gambhir SS, Witte ON. Quantitative imaging of the T cell antitumor response by positron-emission tomography. *Proc Natl Acad Sci U S A* 2003;**100**: 1232-7.
25. Kim D, Hung CF, Wu TC. Monitoring the trafficking of adoptively transferred antigen-specific CD8-positive T cells in vivo, using noninvasive luminescence imaging. *Hum Gene Ther* 2007;**18**: 575-88.
26. Kircher MF, Allport JR, Graves EE, Love V, Josephson L, Lichtman AH, Weissleder R. In vivo high resolution three-dimensional imaging of antigen-specific cytotoxic T-lymphocyte trafficking to tumors. *Cancer Res* 2003;**63**: 6838-46.
27. Su H, Chang DS, Gambhir SS, Braun J. Monitoring the antitumor response of naive and memory CD8 T cells in RAG1-/- mice by positron-emission tomography. *J Immunol* 2006;**176**: 4459-67.
28. Boissonnas A, Combadiere C, Lavergne E, Maho M, Blanc C, Debre P, Combadiere B. Antigen distribution drives programmed antitumor CD8 cell migration and determines its efficiency. *J Immunol* 2004;**173**: 222-9.
29. Schreiber K, Rowley DA, Riethmuller G, Schreiber H. Cancer immunotherapy and preclinical studies: why we are not wasting our time with animal experiments. *Hematol Oncol Clin North Am* 2006;**20**: 567-84.
30. Willimsky G, Czeh M, Loddenkemper C, Gellermann J, Schmidt K, Wust P, Stein H, Blankenstein T. Immunogenicity of premalignant lesions is the primary cause of general cytotoxic T lymphocyte unresponsiveness. *J Exp Med* 2008;**205**: 1687-700.
31. Willimsky G, Blankenstein T. Sporadic immunogenic tumours avoid destruction by inducing T-cell tolerance. *Nature* 2005;**437**: 141-6.
32. Czeh M, Loddenkemper C, Shalapour S, Schon C, Robine S, Goldscheid E, Stein H, Schuler T, Willimsky G, Blankenstein T. The immune response to sporadic colorectal cancer in a novel mouse model. *Oncogene* 2010;**29**: 6591-602.
33. Huettner CS, Zhang P, Van Etten RA, Tenen DG. Reversibility of acute B-cell leukaemia induced by BCR-ABL1. *Nat Genet* 2000;**24**: 57-60.
34. Jonkers J, Berns A. Conditional mouse models of sporadic cancer. *Nat Rev Cancer* 2002;**2**: 251-65.
35. Herzig M, Christofori G. Recent advances in cancer research: mouse models of tumorigenesis. *Biochim Biophys Acta* 2002;**1602**: 97-113.
36. Gajewski TF, Schreiber H, Fu YX. Innate and adaptive immune cells in the tumor microenvironment. *Nat Immunol* 2013;**14**: 1014-22.

37. Anders K, Buschow C, Herrmann A, Milojkovic A, Loddenkemper C, Kammertoens T, Daniel P, Yu H, Charo J, Blankenstein T. Oncogene-Targeting T Cells Reject Large Tumors while Oncogene Inactivation Selects Escape Variants in Mouse Models of Cancer. *Cancer Cell* 2011;**20**: 755-67.
38. Wei S, Shreiner AB, Takeshita N, Chen L, Zou W, Chang AE. Tumor-induced immune suppression of in vivo effector T-cell priming is mediated by the B7-H1/PD-1 axis and transforming growth factor beta. *Cancer Res* 2008;**68**: 5432-8.
39. Charo J, Ciupitu AM, Le Chevalier De Preville A, Trivedi P, Klein G, Hinkula J, Kiessling R. A long-term memory obtained by genetic immunization results in full protection from a mammary adenocarcinoma expressing an EBV gene. *J Immunol* 1999;**163**: 5913-9.
40. Lacroix J, Doeberitz MK. Technical aspects of minimal residual disease detection in carcinoma patients. *Semin Surg Oncol* 2001;**20**: 252-64.
41. Mandl S, Schimmelpfennig C, Edinger M, Negrin RS, Contag CH. Understanding immune cell trafficking patterns via in vivo bioluminescence imaging. *J Cell Biochem Suppl* 2002;**39**: 239-48.
42. Fife BT, Bluestone JA. Control of peripheral T-cell tolerance and autoimmunity via the CTLA-4 and PD-1 pathways. *Immunol Rev* 2008;**224**: 166-82.
43. Gattinoni L, Finkelstein SE, Klebanoff CA, Antony PA, Palmer DC, Spiess PJ, Hwang LN, Yu Z, Wrzesinski C, Heimann DM, Surh CD, Rosenberg SA, et al. Removal of homeostatic cytokine sinks by lymphodepletion enhances the efficacy of adoptively transferred tumor-specific CD8+ T cells. *J Exp Med* 2005;**202**: 907-12.
44. Cheever MA, Allison JP, Ferris AS, Finn OJ, Hastings BM, Hecht TT, Mellman I, Prindiville SA, Viner JL, Weiner LM, Matrisian LM. The prioritization of cancer antigens: a national cancer institute pilot project for the acceleration of translational research. *Clin Cancer Res* 2009;**15**: 5323-37.
45. Crispe IN, Dao T, Klugewitz K, Mehal WZ, Metz DP. The liver as a site of T-cell apoptosis: graveyard, or killing field? *Immunol Rev* 2000;**174**: 47-62.
46. Otto-Duessel M, Khankaldyyan V, Gonzalez-Gomez I, Jensen MC, Laug WE, Rosol M. In vivo testing of Renilla luciferase substrate analogs in an orthotopic murine model of human glioblastoma. *Mol Imaging* 2006;**5**: 57-64.

Figure Legends

Figure 1: T-cell proliferative and homing responses measured by RT-Rack are antigen dependent and can be evoked by small or unpalpable tumor masses. (A) Seven days after injection of antigen-expressing EG.7F (+) and antigen-negative EL-4F (-) tumors cells on opposite sites, tumor-bearing and control tumor-free mice were imaged for tumor signal. (B-C) Mice were then injected with R-OT T cells and imaged 4 days later simultaneously for tumor and T cell signals. (C) Overlay of tumor and T-cell signals is shown in orange. (D-F) Groups of C57BL/6 mice were injected s.c. with EG.7F at 10, 8, 5 or 3 days before T cell injection. (D) Average FLuc tumor signals ± standard deviation from the 4 different groups, 3 days before T cell injection, with their corresponding tumor size at day of treatment indicated at the abscissa. (E) Mice from (D) were either kept untreated (open symbols, no T) or were injected with R-OT T cells (closed symbols, T) and imaged for T cell signal over time. At the treatment day, tumors measured 10 mm (■), 7 mm (♦), 1 mm (▲) in mean diameter or were unpalpable (●). The background signal for FLuc (tumor cells) and RLuc (T cells) is set as abscissa. (F) T cell signal from a representative mouse from each group imaged at day 6 after T cell injection is shown. Images were acquired for 1 min. using medium binning (n=4-5 mice per group). The signal intensity is shown as p/s/cm^2/sr and depicted by a pseudocolor scale.

Figure 2: RT-Rack detects T-cell response to tumors in immunodeficient as well as immunocompetent mice. (A-B) 9.27P s.c. tumor-bearing C57BL/6 (A) and Rag$^{-/-}$ (B) mice as well as tumor-free littermates (control) were injected with R-TCRI T cells or kept untreated and imaged at the indicated days for RLuc activity (T cells). The signal strength is depicted by a pseudocolor scale. Images were acquired for 1 min., using small binning. (C-D) RLuc signal over time at the tumor site (C) or total mouse body (D) of untreated (open symbols, no T) and

T cell treated (closed symbols, T) Rag$^{-/-}$ (■) and C57BL/6 (▲) mice. Data are representative of 2 independently performed experiments (n=4-7 mice per group). The signal intensity is shown as p/s/cm^2/sr and depicted by a pseudocolor scale. (E) Sections from lungs of 9.27P s.c. tumor-bearing Rag$^{-/-}$ and tumor-free littermates (control) were stained for Tag on 4 and 7 days after T cell injection. The photographs are representative of two independently performed experiments. The scale bar corresponds to 100 μm. (F) Seven days after T cell injection, sections of 9.27P tumors from Rag$^{-/-}$ mice were stained for CD8. Shown are the representative photographs of the CD8 staining. CD8 T cell (red) distribution in the tumor is shown in the left panel. The dotted line separates the rim, where the T cells are present, from the necrotic (N) center of the tumor. The scale bar corresponds to 100 μm. The right panel shows the CD8 staining at the rim of the tumor at a higher magnification, with the scale bar corresponding to 25 μm.

Figure 3: RT-Rack detects T-cell response to experimental MCA-TagLuc metastases. (A) Rag$^{-/-}$ mice challenged with MCA205-TagLuc cells were imaged for FLuc activity to detect metastases formation. Shown is tumor signal over time and change in FLuc (tumor) signal (p/s) from the lung area of the mouse is plotted in the graph. (B) One day before T cell injection (4 days after injection of MCA205-TagLuc cells), mice were imaged for FLuc activity to detect the metastases. On treatment day, mice received R-TCRI T cells. (C) RLuc activity was measured on days 2-6. Shown are two representative mice with either uni- or bilateral metastases. (D) T cell signal in the lung over time from tumor bearing (closed symbol, n=6) and tumor free (open symbol, n=1) mice. (E-F) 6 days after T cell transfer, mice were sacrificed and the lungs were imaged *ex vivo* for RLuc activity (F). As a control, one mouse without T cell treatment was sacrificed at the same time and the lung was imaged for FLuc activity (E). (G) Rag$^{-/-}$ mice with MCA205-TagLuc tumors (Tag +, n=5) or MCA205-

MigFLuc tumors (Tag -, n=3) or without tumor (negative control, n=5) were injected with R-TCRI T cells. RLuc activity was measured 6 days later. Images were acquired for 1 minute using small binning. (H) Mice in (G) were sacrificed and the lungs were imaged *ex vivo* for RLuc activity. Data summarize one representative out of 2 independently performed experiments. The signal intensity is shown as p/s/cm^2/sr and depicted by a pseudocolor scale.

Figure 4: RT-Rack detects the T-cell response to Cre recombinase-induced liver tumors in LTL x Alb-Cre mice. (A) 4-6 months old LTL x Alb-Cre mice (double transgenic, single transgenic and wild type mice) were imaged for FLuc to visualize tumor presence (1 second, small binning). In addition, single transgenic mice were imaged for 1 minute to visualize the leakiness reported to be detected in LTL mice. (B) Mice imaged in (A) were injected with R-TCRI T cells and imaged at the indicated days for RLuc activity. (C) At day 7, mice were also imaged for both FLuc and RLuc signals simultaneously. A double transgenic mouse (left panel) and an Alb-Cre - single transgenic mouse (right panel) are shown. Top panels show RLuc signal (T cells) and middle panels FLuc signal (liver tumor). The overlay of both signals results in orange color and is shown in the bottom panels. (D-E) Liver (D) or total body (E) RLuc signal over time of Alb-Cre x LTL (♦), Alb-Cre (■), LTL (◇) and wild type (□) littermate mice. The experiment is representative of 2 independently performed experiments. (F) 4-6 months old LTL x Alb-Cre mice were imaged for FLuc activity twice 12 days apart (d-24 and d-12, on 24 and 12 days before T cell injection.) to visualize tumor presence and progression. An Alb-Cre single transgenic mouse was used as a negative control. (G) At day 0, LTL x Alb-Cre mice from (F) were injected with R-TCRI T cells and imaged for RLuc activity at the indicated days post T cell transfer. Images were acquired for 1 minute, using small binning. (H) Graph showing the correlation between tumor burden (Fluc signal

from (F) on day -12) and T cell accumulation (RLuc signal from (G) on day 4). The signal intensity is shown as p/s/cm^2/sr and depicted by a pseudocolor scale.

Figure 5: RT-Rack based on the usage of TCR I transduced T cells detects T-cell response against Tag expressing tumors. (A) R-OT T cells were retrovirally transduced to express the Tag specific TCR I or were mock transduced with pMIG. Transduction rate was measured one day following the last transduction (at the day of T cell injection) with D^b-peptide I multimer (TCR I) or for GFP (pMIG). Cells were costained for CD8. (B) Rag$^{-/-}$ mice were challenged with 16.113F tumor cells s.c. and were injected 49 days later with 10^5 OT-I-ChRLuc T cells transduced with TCR I (n=5) or pMIG (n=2) as a negative control and imaged for RLuc activity (T cells) at the indicated days. Images were acquired for 1 minute using small binning. (C) T cell signal over time from tumor sites. Data represent the summary of one representative out of 2 independently performed experiments. The signal intensity is shown as p/s/cm^2/sr and depicted by a pseudocolor scale.

Figure 6: TILs from LTL mice have less functional and more exhausted phenotype than TILs from Rag$^{-/-}$ or C57BL/6 mice. Two weeks after 9.27P tumor challenge, Rag$^{-/-}$ (■), LTL (▥) and C57BL/6 (□) mice were injected with R-TCRI T cells. After 7 days, splenocytes or TILs were isolated and analyzed for PD1 expression and the ability to respond to antigen-specific stimulation by flow cytometry. Shown are bar graphs summarizing the percentage of PD1 expression (A-C) and the MFI of PD1$^+$ cells from (A-C) in CD8$^+$ Vβ7$^+$ from TILs (A, D) and splenocytes (B,C, E andF) ex vivo. (G-J) Cells from A-F were stimulated *in vitro* with peptide I of Tag. Shown are graphs summarizing the percentage of CD8$^+$ Vβ7$^+$ among TILs (G, J) and splenocytes (H-I) secreting IFN-γ (G-I) or granzyme B (J). Splenocytes from tumor-free littermates were used as control (C, F, I). TILs and splenocytes restimulated with gp33 as negative control did not secrete IFNγ or granzyme B (data not

schown). The experiments are representative of 2 independently performed sets of experiments.

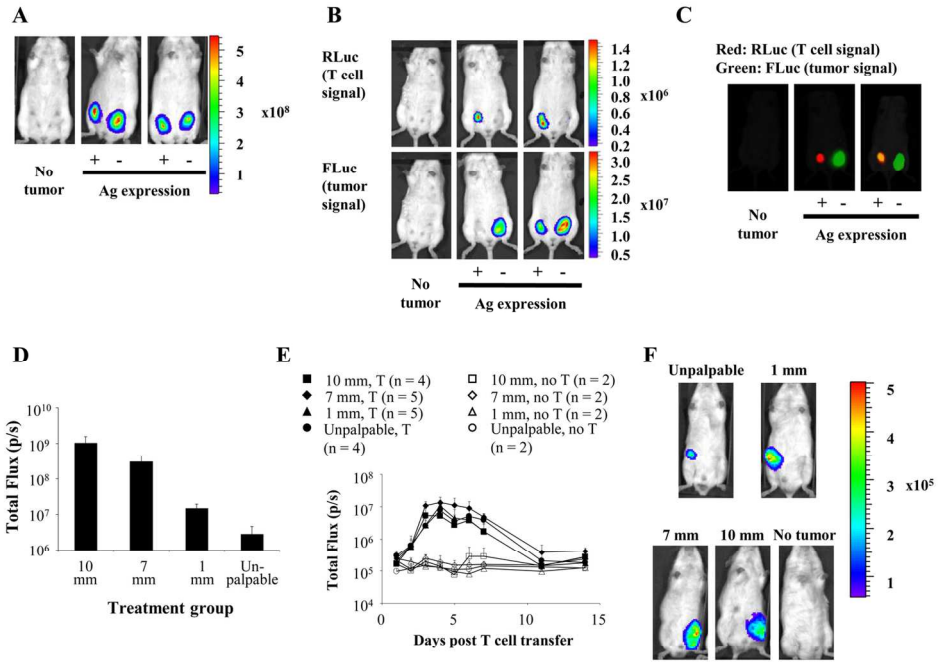

Figure 1
140x106mm (300 x 300 DPI)

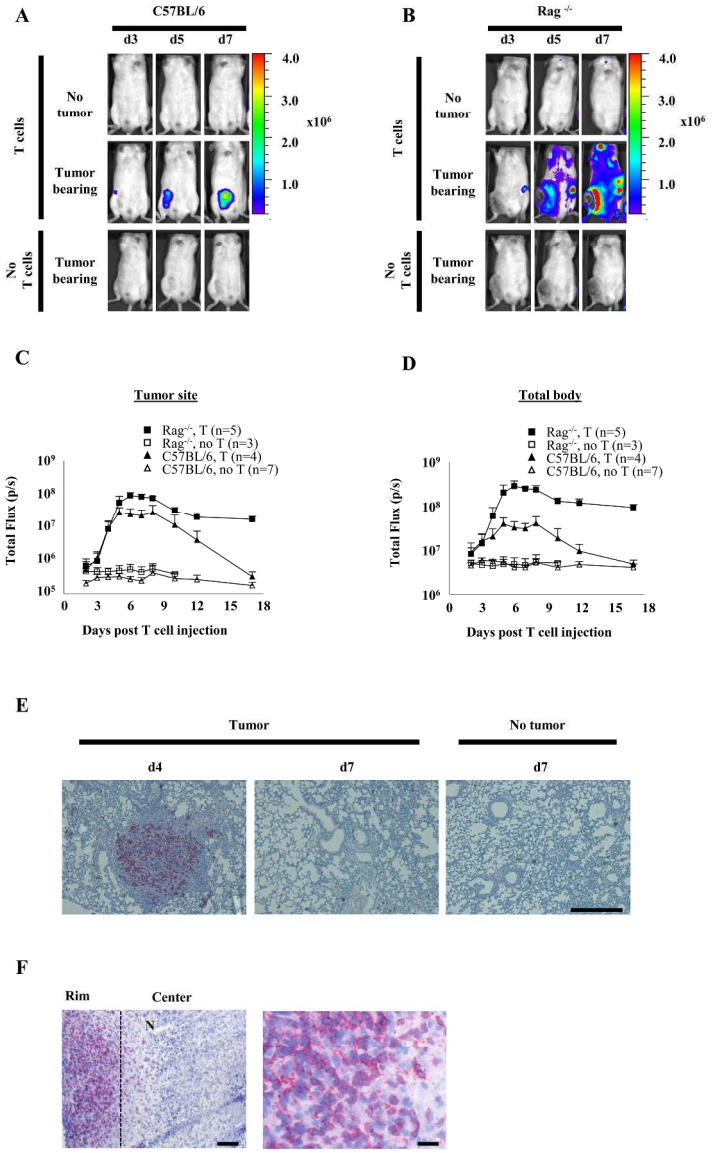

Figure 2
249x407mm (300 x 300 DPI)

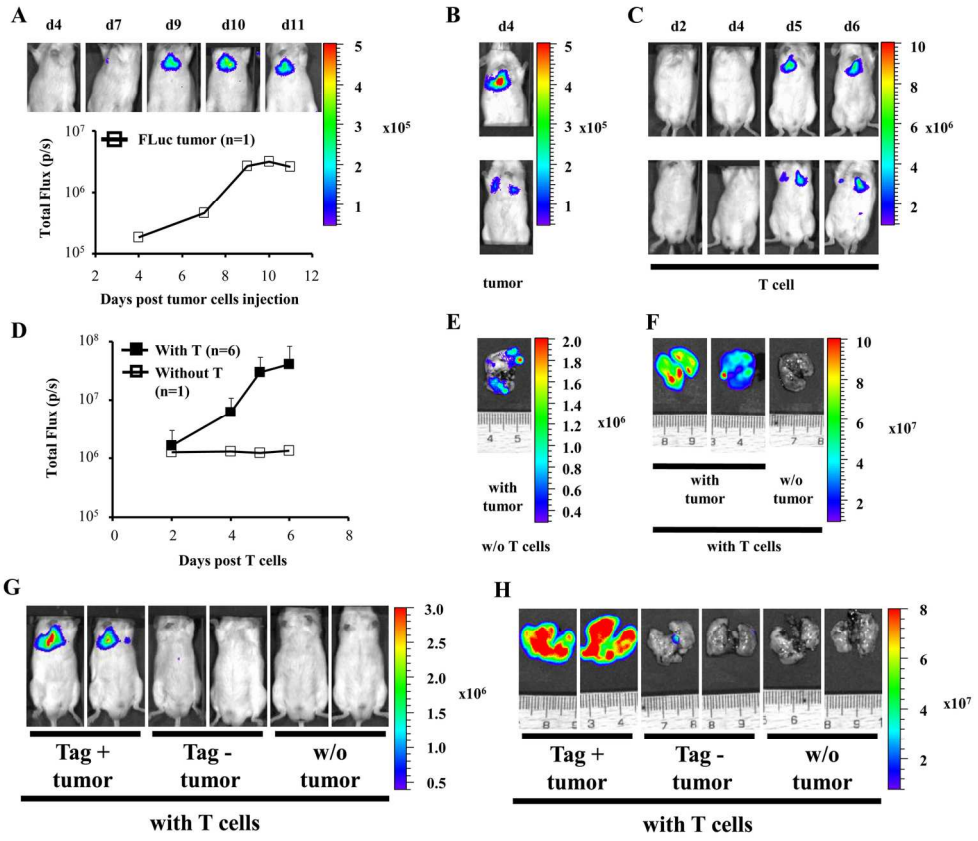

159x136mm (300 x 300 DPI)

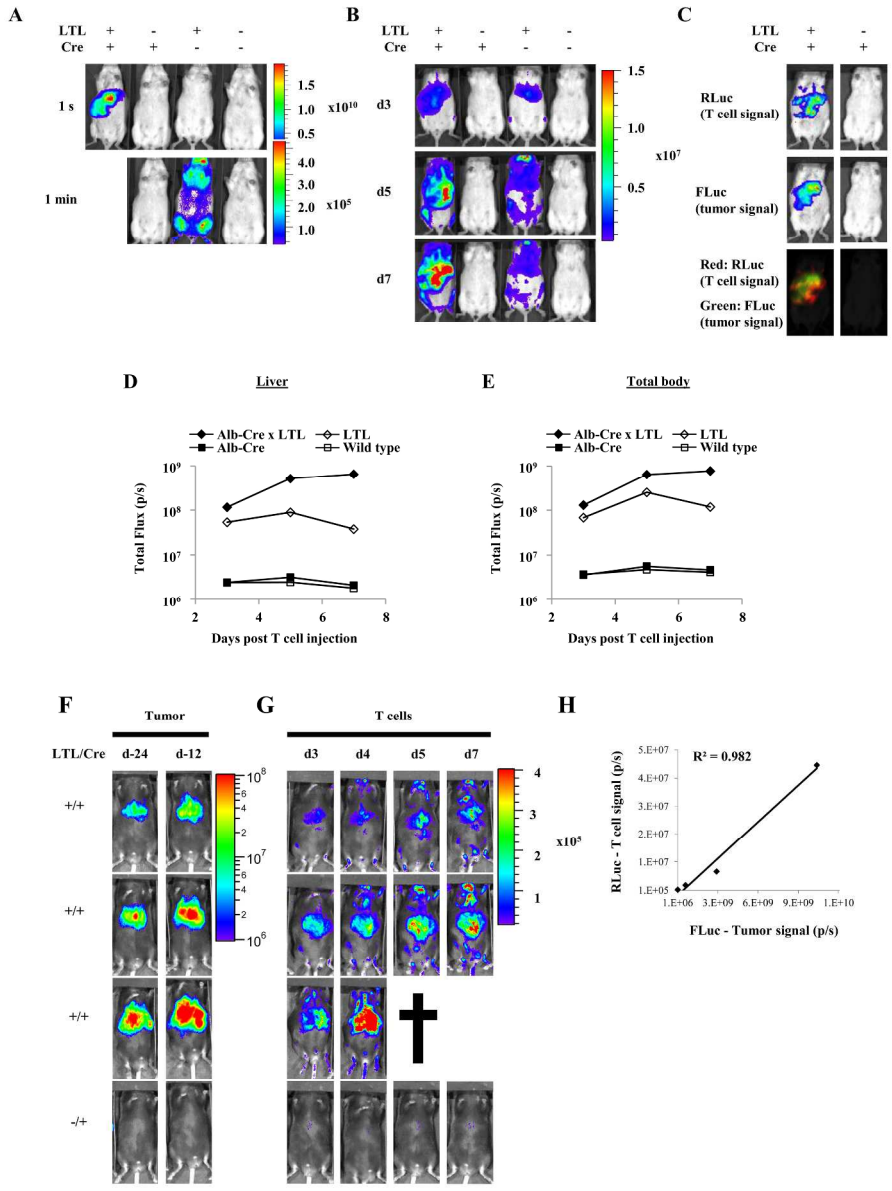

248x333mm (300 x 300 DPI)

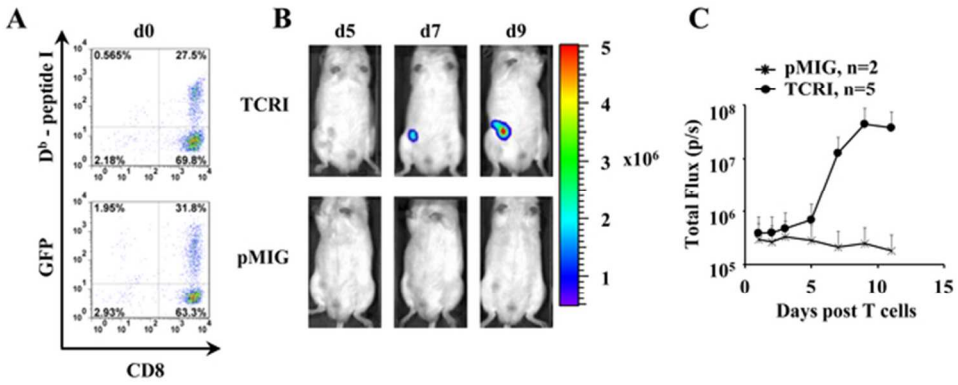

58x24mm (300 x 300 DPI)

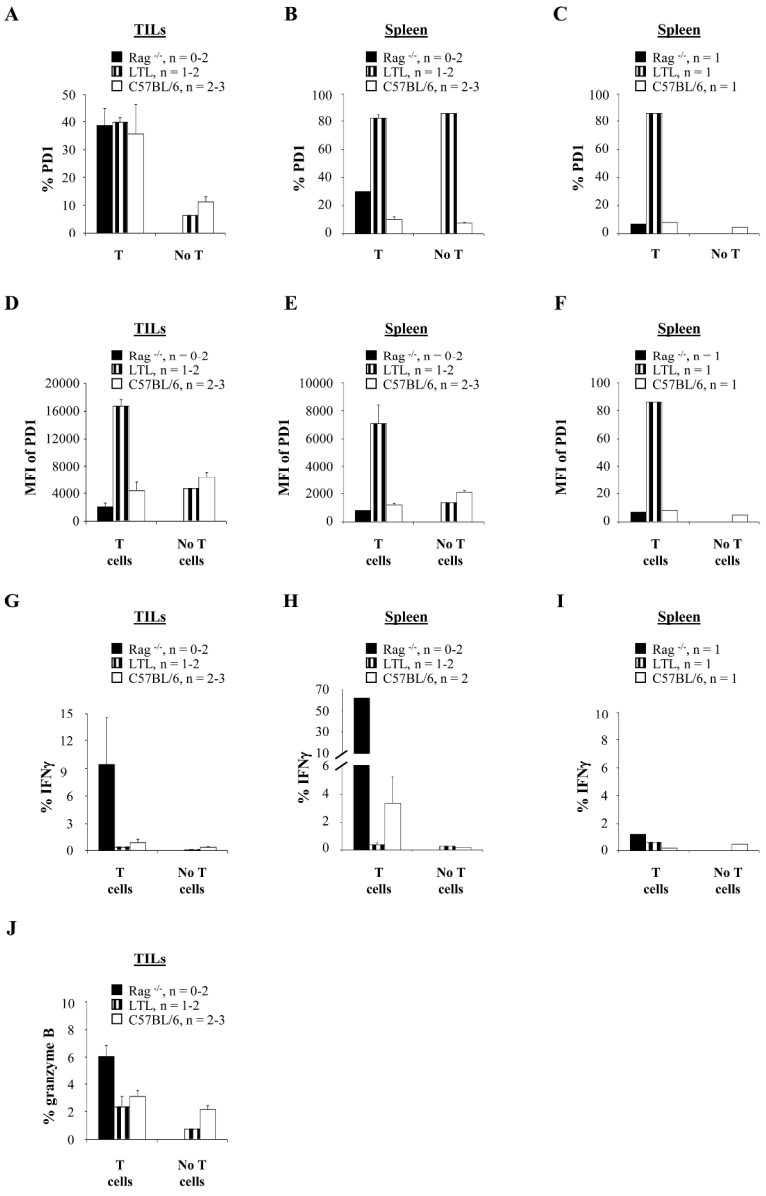

249x366mm (300 x 300 DPI)